Redesigning the Topology of a Four-Helix-Bundle Protein: Monomeric Rop†

Paul F. Predki and Lynne Regan*

Department of Molecular Biophysics and Biochemistry, Yale University, New Haven, Connecticut 06520

Received May 2, 1995; Revised Manuscript Received June 2, 1995®

ABSTRACT: The topology of α-helices and β-sheets in folded proteins is largely specified by the connectivities of the loops and turns which join them. We have used the protein Rop to test the feasibility of using short glycine-rich linkers to reconnect the α-helices within a four-helix-bundle protein. In wild-type Rop the four-helix-bundle structure is formed by the association of two identical helix−turn−helix monomers. Our redesigns encode Rop as a single chain to create a monomeric, rather than a dimeric, form of the protein. Characterization of a series of such variants demonstrates that new connections of this type can be used to generate stable, native-like proteins. The length of the connections is of key importance: if the loops are too short, correct association of the helices is prevented, and misfolded, higher order oligomers occur. Designs with sufficiently long loop connections, however, generate exclusively the desired monomeric form of the protein. Moreover, the successful monomeric designs bind Rop's RNA substrate with affinities that are equal to that of the wild-type protein. This result provides strong confirmation that the positioning of the helices in the monomeric variants is closely similar to that in wild-type Rop.

The four-helix bundle is a commonly occurring structural motif typified by an antiparallel arrangement of four α-helices that cross at an angle of about 20° (Presnell & Cohen, 1989). The helices are linked by loops which can vary dramatically in their length, sequence, and connectivity. Loop connections range from short, direct, tight turns to long "overhand" extended loops. The basic four-helix-bundle framework can support a diverse variety of activities, from oxygen transport in myohemerythrin to receptor binding in the hematopoietic growth factors and RNA binding in Rop. The ability to redesign the topology of proteins in general, and of four-helix-bundle proteins in particular, is of interest for a number of reasons. Of potential practical importance, for example, would be redesigns of therapeutically important proteins that retain the essential elements of the proteins' functionality, but on a simplified and more stable framework. In addition, remodeling a dimeric protein into a monomeric form could simplify studies of the effects of single amino acid changes (rather than double changes in the dimeric versions) on protein structure, function, and folding. Finally, development of effective methods to link elements of secondary structure is essential for the progress of *de novo* protein design.

Related protein redesigns, which had somewhat different aims, have been achieved in the creation of single-chain antibodies (Bird et al., 1988), fusions of two or more protein domains (Toth & Schimmel, 1986; Bizub et al., 1991; Liang et al., 1993; Bovia et al., 1994), and designs for circularly permuted forms of proteins such as BPTI (Goldenberg & Creighton, 1983), yeast phosphoribosyl anthranilate isomerase (Luger et al., 1989) T4 lysozyme (Zhang et al., 1993), β-glucanase H (Hahn et al., 1994), and a recombinant interleukin 4 toxin (Kreitman et al., 1994). However, in the above examples the new connectivies largely involve joining pre-existing N- and C-termini which are already close together in space. In the case of the circularly permuted variants, new N- and C-termini were created by starting and terminating the chain at internal positions in the protein. The goal of our designs is somewhat different. Our aim is to reconnect secondary structural elements at positions which are internal to the sequence of a protein. Consequently, the constraints on the successful realization of such designs are more severe than those in which intact protein domains are linked.

The RNA-binding protein Rop serves as an ideal model system for our redesign efforts. Rop is a simple, dimeric, four-helix-bundle protein formed by the association of two identical helix−turn−helix monomers. The structure of the wild-type protein is known at high resolution (Banner et al., 1987), its interaction with an RNA substrate is well characterized (Eguchi & Tomizawa, 1990, 1991; Predki et al., 1995), and the thermodynamic properties of the wild-type protein are well described (Steif et al., 1993; Munson et al., 1994b).

We note that several years ago a design for a single-chain variant of Rop was presented (Sander, 1990). In this design the helices were connected in the order 1−2−2′−1′, using loop connections derived from a database search. However, experimental verification of the success or failure of this design has yet to be reported. Our designs differ from this earlier design in two important ways. First, the order of helix connections is different; in our design the helices are connected 1−1′−2′−2 (see the results section for a detailed discussion of the rationale behind this design). Second, the loops we use are of the simplest sequence complexity; this allows the effect of loop length to be studied in a systematic fashion.

† This work was supported by NIH Grant GM49146. L.R. is an NSF National Young Investigator. P.F.P. is an MRC (Canada) Post-Doctoral Fellow.

® Abstract published in *Advance ACS Abstracts,* July 1, 1995.

0006-2960/95/0434-9834$09.00/0

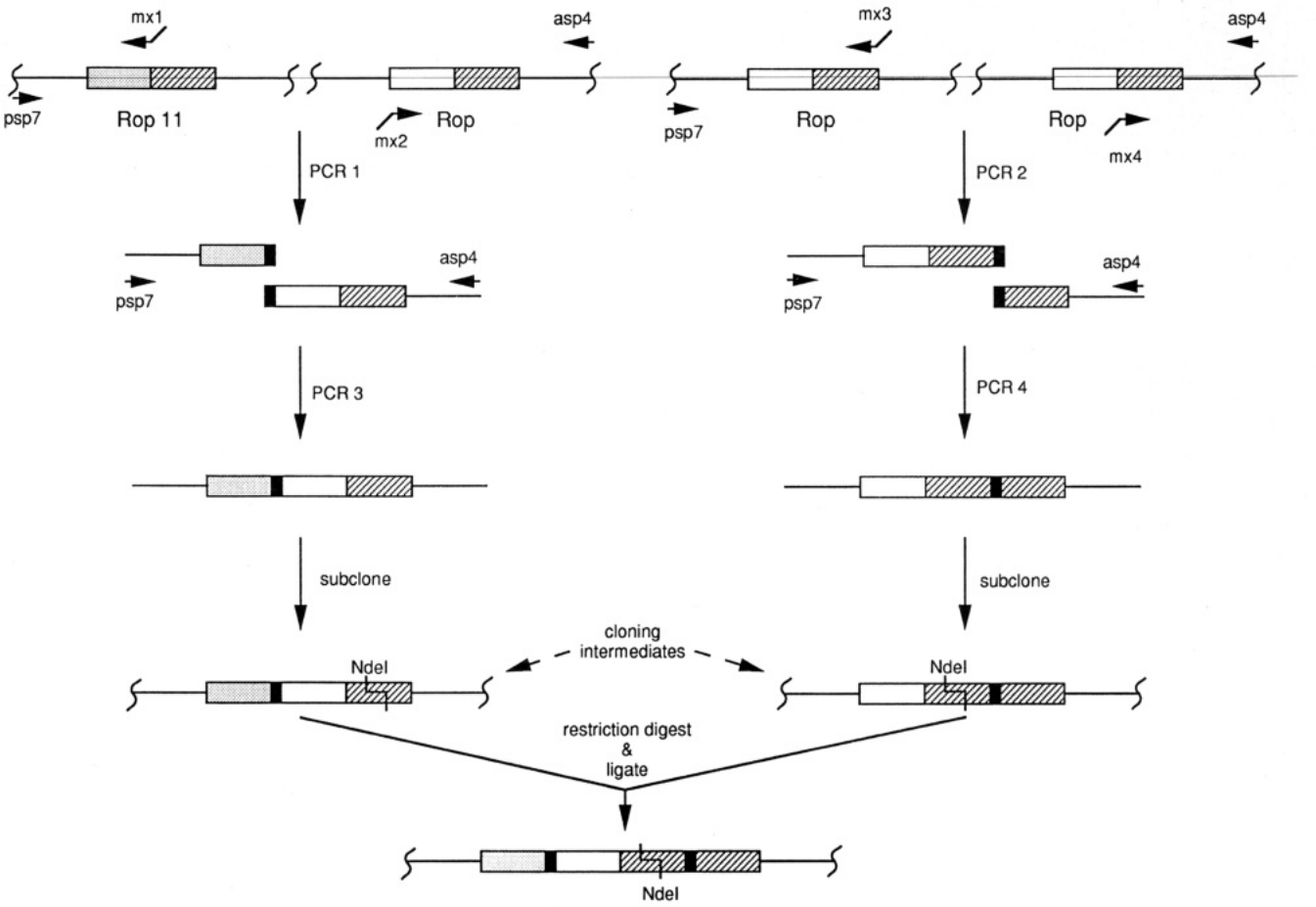

FIGURE 1: Schematic illustration of the PCR cloning strategy. The DNAs encoding Rop11 (wild-type DNA sequence) and Rop (non-wild-type redundant DNA sequence) helices 1, 2, 1′, and 2′ are represented by the shaded, open, and hatched boxes. Glycine inserts are represented by filled boxes, and flanking DNA sequences are represented by lines. PCR primers psp7, mx1, mx2, mx3, mx4, and asp4 are depicted by arrows. A detailed description of the cloning methodology is presented in Experimental Procedures.

EXPERIMENTAL PROCEDURES

Mutagenesis and Cloning. The single-chain versions of Rop were created using the PCR-based[1] cloning strategy illustrated in Figure 1. Two plasmids encoding wild-type Rop were available to us: pMR101-Rop11, in which wild-type Rop is encoded by the wild-type DNA sequence (Rop11) (Munson et al., 1994a), and p2R (Predki et al., 1995), in which wild-type Rop is encoded by a different DNA sequence, using degenerate codons. Thus, the Rop gene in p2R has an altered restriction pattern relative to that of the Rop gene in pMR101-Rop11. Initial PCR half-reactions used primers with complementary 5′ overhangs encoding the desired number of glycine residues in the loop. The PCR half-reaction involving helix 1 was performed using the Rop gene encoded by pMR101-Rop11 as template, while other half-reactions utilized the p2R vector. The names and positions of the primers used are also shown in Figure 1. The mx4 primers were additionally designed to remove the *Nde*I site on helix 2. Initial half-reaction products from PCRs 1 and 2 (Figure 1) were excised from 2.5% low-melt agarose gels and melted for subsequent PCR reactions (3 and 4) with flanking primers psp7 and asp4. These PCR products were then restriction digested as indicated in Figure 1 and inserted into similarly digested pMR103-RopD30G. This plasmid encodes a variant of wild-type Rop that carries the D30G stabilizing point mutation (P. F. Predki and L. Regan, manuscript in preparation). The various single-chain Rops were generated by combing the appropriate cloning intermediates using unique *Nde*I sites internal to the gene and a *Pst*I site within the vector. Using this strategy, the single-chain Rops contain several diagnostic restriction sites within helices 1 and 2 which are absent in helices 1′ and 2′ (not shown). All sequences were confirmed by the dideoxy DNA sequencing method (Sanger et al., 1977).

Protein Expression and Purification. Rop variants were purified from *Escherichia coli* strain BL21 (DE3) to greater than 98% purity, as estimated from Coomassie blue stained SDS−polyacrylamide gels. The purification was performed essentially as described previously (Munson et al., 1994b), except sodium phosphate, pH 7.0, was used in place of Tris-HCl during ion-exchange chromatography. Final concentrated protein stocks were prepared using Centriprep 3 microconcentrators (Amicon), followed by dialysis at 4 °C against 10 mM sodium phosphate, pH 7.0, and 350 mM NaCl buffer.

RNA Binding Assay. To assay RNA-binding activity, electromobility shift assays were performed as described (Predki et al., 1995), except that the gels and running buffer contained 5 mM $MgCl_2$ and 45 mM Tris−borate. Dissociation constants (K_d) were calculated, assuming simple 1:1 binding, using the equation $K_d = [Rop^f][RNA^f]/[Rop{\cdot}RNA]$,

[1] Abbreviations: CD, circular dichroism; DTT, dithiothreitol; K_d, dissociation constant; PAGE, polyacrylamide gel electrophoresis; PCR, polymerase chain reaction; SDS, sodium dodecyl sulfate; T_m, melting temperature.

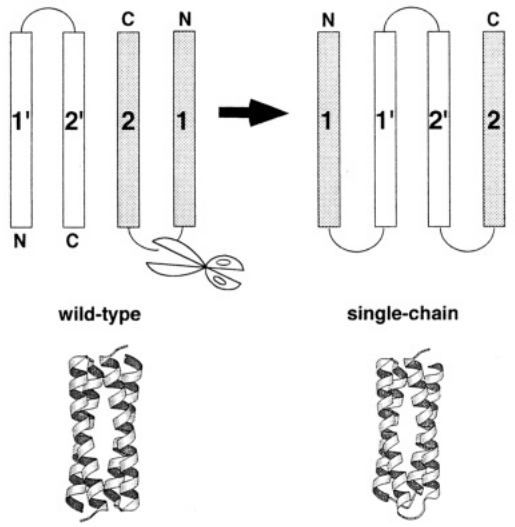

FIGURE 2: Topology redesign strategy. A schematic illustration of the relative topology of wild-type Rop and the monomeric variants is depicted in the upper panels. In the lower panels, ribbon drawings [created using the program Molscript (Kraulis, 1991)] of wild-type Rop and the model for the monomeric Rop_{S44} variant are shown.

where [Rop^f] is the concentration of free protein, [RNA^f] is the concentration of free RNA, and [Rop•RNA] is the concentration of the protein−RNA complex. Values for [RNA^f] and [Rop•RNA] were obtained by quantification of the appropriate bands on a FUJI BAS2000 phosphorimager using MacBAS v1.01 software. Since the total concentration of Rop added to the assay, [Rop^t], is known, [Rop^f] is calculated from the relationship [Rop^t] = [Rop^f] + [Rop•RNA]. Estimated error in K_d values is ±10%.

Gel Filtration Analysis. Gel filtration analysis was performed at 4 °C with ~100 μg of protein on a Pharmacia Superdex75 16/60 gel filtration column equilibrated with a 10 mM sodium phosphate, pH 7.0, and 350 mM NaCl buffer. A flow rate of 1.0 mL/min was used, and elution was monitored by absorbance at 214 nm. The relative amounts of monomeric and oligomeric species were quantified by determining the areas under the elution peaks.

CD Spectroscopy. CD measurements were recorded on an AVIV Model 62DS circular dichroism spectrometer (AVIV Instruments, Lakewood, NJ) running Aviv software. CD spectra and thermal denaturation curves for Rop were performed on 1.5−23 μM protein samples in 10 mM sodium phosphate (pH 7) and 350 mM NaCl. For thermal denaturations, 1 mM DTT was also used. Thermal denaturation was monitored at 222 nm over the range 20−98 °C, using a temperature step size of 1 °C, a 2-min equilibration period, and a 1-min signal averaging time. Under these conditions the thermal denaturation transition of wild-type and monomeric Rop is fully reversible (data not shown). We note, however, that extended exposure to high temperatures (>85 °C) results in aggregation of Rop_{S44} at elevated protein concentrations. Prolonged incubation under these conditions was therefore avoided. After correction of thermal denaturation profiles by subtraction of both lower and upper baselines, T_ms were determined by interpolation. These calculations were performed using the computer program ThermoDynaCD, written by P.F.P.

Model Building. The molecular model for monomeric Rop depicted in Figure 2 was built by inserting two Gly_4 turns into the structure of wild-type Rop in the appropriate locations using the program Sybyl (Tripos Associates Inc.). This structure was then subjected to a 500-step conjugate gradient energy minimization. After this, a 100-ps molecular dynamics slow cooling stage (2000 to 300 K) followed by 20 ps of constant temperature dynamics (300 K) was employed. The resulting structure was further energy minimized using a final 300-step conjugate gradient minimization. All molecular dynamics and energy minimization steps were performed using X-PLOR (Brunger, 1992) with the CHARMM PARAM19 parameter set. During molecular dynamics calculations, the positions of all residues except those in the glycine turns were held fixed.

RESULTS

Design of the Single-Chain Rop Variants. The RNA-binding determinants in wild-type Rop are located on the solvent-exposed surface of the helix 1/1′ face of the protein. By contrast the exposed helix 2/2′ surface has no residues that are involved in direct interactions with RNA (Predki et al., 1995). Because our aim was to design single-chain variants that retain RNA-binding activity, one consideration in the placement of the connecting loops was to have helix 1 and helix 1′ directly connected. Two additional features were incorporated into the design. First, in an attempt to enhance the stability of the single-chain Rops, the stabilizing mutation D30G was incorporated into the "wild-type" turn which connects helices 1 and 2. In previous studies we have demonstrated that the D30G substitution enhances the T_m of wild-type Rop by 13 °C and the free energy of folding by approximately 2 kcal mol^{-1}, at a protein concentration of 15 μM (P. F. Predki and L. Regan, manuscript in preparation). Second, earlier studies had indicated that the six C-terminal amino acids of wild-type Rop, which extend beyond helix 2/2′ as an unstructured tail, are in fact required to maintain high protein solubility (Smith et al., 1995). To preserve this feature of the protein, the helices were connected in the order 1−1′−2′−2, such that the tail was retained after helix 2. This design preserves the natural N- and C-termini of the protein. Also note that one end of the protein maintains native connectivity, while both of the designed loops are at the opposite end (Figure 2).

The loop connections were designed as follows: residue L29 of helix 1 is connected to residue T2 of helix 1′, and residue F56 of helix 2′ is connected to residue A31 of helix 2, by the designed loops of varying length (numbering refers to the wild-type sequence). Glycine residues were chosen for the loop sequences to take advantage of its large range of permissible backbone dihedral angles. When modeled using the X-ray crystal structure coordinates of wild-type Rop, the distance between the α-carbon of L29 on helix 1 and the α-carbon of residue T2 on helix 1′ is 10.4 Å. The comparable distance separating the α-carbon of F56 on helix 2′ and the α-carbon of T2 on helix 1′ is 9.43 Å. As a minimal estimate we judged three glycine residues, in an extended conformation, could be sufficient to form new connecting loops. Our aim was to design the shortest possible loop connections, to avoid the potentially destabilizing entropic cost associated with long loops. Therefore, in the initial construct, two loops each consisting of three glycine residues were incorporated to generate Rop_{S33} (*S* for single-chain, with 3 glycine residues in loop 1 (which connects helix1 and helix1′) and 3 glycine residues in loop 2 (which connects helix 2 and helix2′).

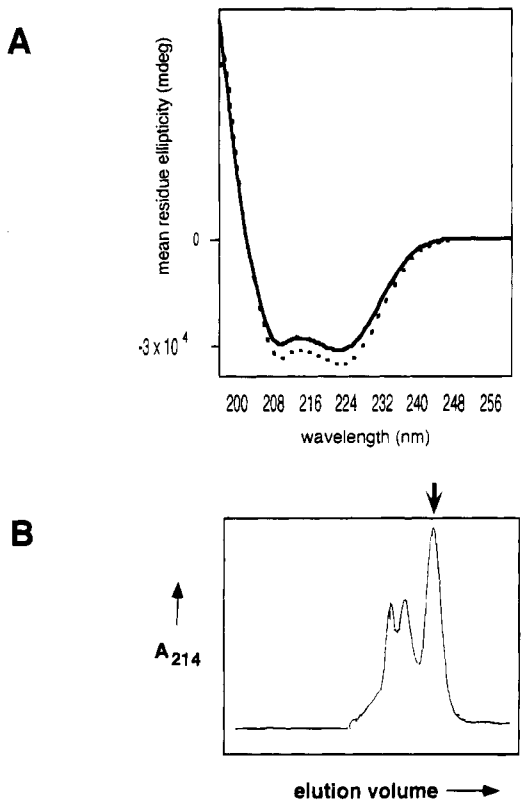

FIGURE 3: CD and gel filtration analysis of Rop_{S33}. (A) Mean residue ellipticity is plotted as a function of wavelength. The spectrum of Rop_{S33} is plotted as a solid line, and that of wild-type Rop is plotted as a dashed line. Spectra were recorded with ~10 μM protein samples in 10 mM phosphate (pH 7.0) and 350 mM NaCl. (B) Gel filtration elution profile of Rop_{S33}. Absorbance at 214 nm is plotted against elution volume. Wild-type Rop elutes at the location indicated by the arrow.

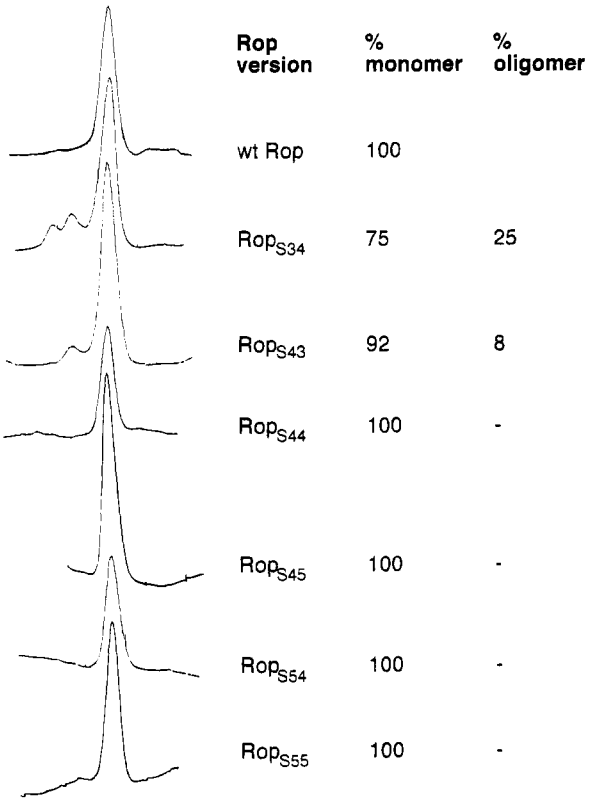

FIGURE 4: Gel filtration analysis of the single-chain Rops vs wt Rop. Typical elution profiles (absorbance at 214 nm plotted against elution volume) for the various proteins are shown on the left. Estimates of the percent protein in monomeric and oligomeric forms, based on the areas of the peaks in the gel filtration profiles, are listed on the right. In all cases the protein was chromatographed directly as obtained after purification from *E. coli*. Therefore, for variants for which multiple species are observed, the distribution does not necessarily reflect a unique equilibrium distribution.

Characterization of Rop_{S33}. Our initial characterization of Rop_{S33} was to compare its CD spectrum with that of wild-type Rop. The CD spectrum of Rop_{S33} was indicative of high α-helical content, and appeared similar to that of the wild-type protein (Figure 3). More detailed characterizations, however, revealed that the high helical content we observed for Rop_{S33} was not diagnostic of a completely sucessful design.

In the second stage of characterization of Rop_{S33}, gel filtration chromatography was employed to assess the overall size and shape of the protein. Rop_{S33} elutes in multiple peaks from a Superdex75 16/60 (Pharmacia) gel filtration column (Figure 4) and similarly migrates as multiple bands on native PAGE (data not shown). These observations suggested that Rop_{S33} may exist in several slowly interconverting forms, a conclusion that is supported by the observation that the relative amounts of the different species change upon incubation of the protein at elevated temperature. We believe that the additional species represent higher order oligomers that are formed in addition to the designed monomeric form. The existence of the higher order species suggested that the Gly_3 loops may be too short. Although the protein is able to fold into a monomeric form (about 50% monomer in the distribution), strain induced by the short loops could favor an opening up of the structure, exposing hydrophobic residues which can enhance the tendency for aggregation. We note that a similar argument has been proposed to explain apparent formation of trimer, rather than dimer, in a *de novo* designed helical protein (Ho & Degrado, 1987). With Rop_{S33}, the open, elongated structures could associate with other similar structures in a variety of ways, giving rise to the multiple species we observe. In an attempt to circumvent this problem, we created additional single-chain versions of Rop with longer loop connections.

Characterization of Rop Variants with Longer Loop Connections. (A) Gel Filtration Chromatography. To systematically investigate the effect of loop length on protein structure and stability, six additional single-chain Rop variants were created. Rop_{S34} and Rop_{S43} have one Gly_3 loop and one Gly_4 loop, Rop_{S44} has two Gly_4 loops, Rop_{S45} and Rop_{54} have one Gly_4 and one Gly_5 loop, and Rop_{S55} has two Gly_5 loops. Characterization of these proteins confirmed our hypothesis that the short loop length was responsible for incorrect folding and the resulting heterogeneity observed with Rop_{S33}. Figure 4 shows gel filtration chromatographs of all the single-chain Rop variants. It is clear that while Rop_{S33} is only about 50% monomeric form, Rop_{S34} and Rop_{S43} are 75% and 92% monomeric, respectively. The difference between Rop_{S34} and Rop_{S43} suggests that although Gly_3 loops are too short in both positions, the Gly_3 loop between helix 1 and helix 1′ has a more severe effect. The construct Rop_{S44}, with two Gly_4 loops, is entirely monomeric, as are Rop_{S45}, Rop_{S54}, and Rop_{S55}.

Finally, we note that, for equal amounts of protein loaded, the gel filtration elution profiles of the successful monomeric Rop designs have line widths at half-height that are identical to that observed for wild-type Rop. This observation

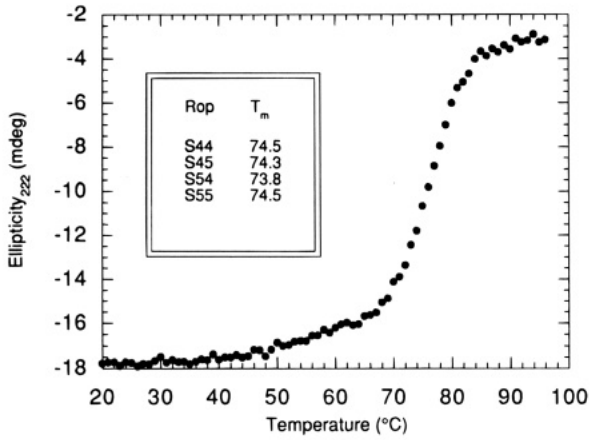

FIGURE 5: Thermal denaturation of Rop_{S44}. CD ellipticity at 222 nm is plotted as a function of temperature. The inset lists the melting temperatures of the 100% monomeric Rop variants. The estimated error in the melting temperatures is approximately ±0.5 °C. The van't Hoff enthalpies of unfolding at T_m (ΔH_{T_m}) are −67, −65, −62, and −69 kcal mol^{-1} for Rop_{S44}, Rop_{S54}, Rop_{S45}, and Rop_{S55} respectively. The estimated error in ΔH_{T_m} is ±10%.

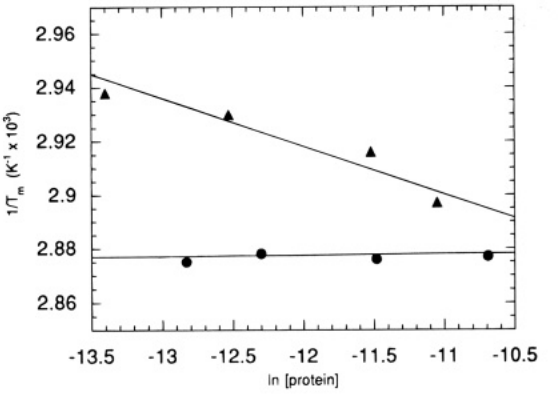

FIGURE 6: Concentration dependence of the melting temperature of wild-type Rop and Rop_{S44}. Melting temperatures for both wildtype (▲) and Rop_{S44} (●) were determined as described in Experimental Procedures at a variety of protein concentrations (1.5 × 10^{-6} to 1.6 × 10^{-5} M for wild-type; 2.7 × 10^{-6} to 2.3 × 10^{-5} M for Rop_{S44}). $1/T_m$ is plotted against the ln[protein].

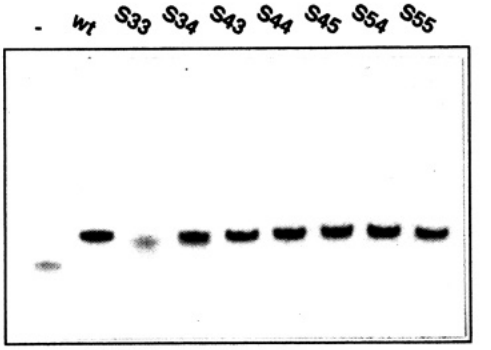

FIGURE 7: Electrophoretic mobility shift assay of RNA binding. The first lane is the RNA alone; the remaining lanes are RNA in the presence of a saturating concentration (10 μg) of the indicated protein.

suggests that wild-type Rop and the monomeric variants are each homogeneous species.

(B) Stability of the Monomeric Rop Variants. The gel filtration behavior of the single-chain Rop variants with loop connections of four or more Gly residues provided the first evidence that the proteins were folding into a unique monomeric species. It was also important to determine the stabilities of the redesigned proteins and to compare their structures in a more rigorous fashion. Figure 5 shows a representative thermal denaturation curve for Rop_{S44}. The thermal denaturation transition is cooperative with a significant associated enthalpy of unfolding, suggesting that the redesigned protein reproduces the native-like properties of a natural protein. The high melting temperature of Rop_{44} (74.5 °C) suggests that the designed loops allow the protein to adopt a stably folded structure. The other successful single-chain designs, Rop_{45}, Rop_{54}, and Rop_{45}, behave similarly, and also have melting temperatures of about 74 °C (Figure 5, inset). When the stability of the proteins was compared by denaturation with GuHCl, they were all found to be more stable than the wild type and of approximately equally stability to each other (data not shown).

As an additional test of the monomeric state, the melting temperature of one of the proteins, Rop_{S44}, was determined at a variety of protein concentrations (Figure 6). The melting temperature of Rop_{S44} is independent of protein concentration over a 10-fold range, consistent with the proposed monomeric structure of the protein. For comparison, the concentration dependence of the melting temperature of wild-type Rop is also shown. In this case, the melting temperature of the protein increases with increasing concentration. As expected for a dimeric protein, a plot of $1/T_m$ (K^{-1}) vs ln[protein] yields a straight line (Steif et al., 1994).

(C) RNA-Binding Properties of the Monomeric Rop Variants. The natural role of Rop *in vivo* is to bind to an RNA complex as part of the copy-number regulatory mechanism of ColE1 plasmids (Polisky, 1988). Rop's RNA-binding activity can be assayed *in vitro* using an electrophoretic mobility shift assay with small RNA hairpin substrates (Gregorian & Crothers, 1995; Predki et al., 1995). The RNA-binding assay thus provides a sensitive means by which to assess the structural integrity of the single-chain Rop variants. Figure 7 shows a comparison of the RNA-binding properties of wild-type Rop and the single-chain Rop variants. The electrophoretic mobilities of the wild-type Rop−RNA complex and those of the monomeric Rop designs are identical, suggesting that the proteins bind RNA in the same fashion.

Note that although all single-chain variants are able to bind the RNA complex, Rop_{S33} and, to some extent, Rop_{S34} are smeared out. This suggests that with these proteins the bound complexes may be dissociating during the electrophoretic run, implying a lower affinity for the RNA. Since both Rop_{S33} and Rop_{S34} consist of a mixture of monomeric and oligomeric forms, it is not possible to calculate a meaningful dissociation constant for RNA binding. However, in the case of the fully monomeric Rop_{S44} a dissociation constant can be measured (see Experimental Procedures for details). The apparent dissociation constant of Rop_{S44} is 1.4 × 10^{-6} M, comparable to the 0.8 × 10^{-6} M value for wild-type Rop measured under these conditions. The similarity of the RNA-binding affinities of Rop_{S44} and wild-type Rop indicates that the introduction of the two Gly_4 turns in Rop_{S44} does not significantly alter the global structure of the protein and that the relative positioning of the helices is maintained.

DISCUSSION

The results presented here demonstrate the feasibility of altering a protein's topology and converting a dimeric protein into a monomeric protein using simple glycine linkers. Our

results also show that in Rop, if the loop connections are too short, alternative, although still highly helical, oligomeric structures can be formed. We demonstrate that this alternative folding scheme can be avoided if the length of the connecting loops is increased. In the case of Gly_4, the loops are sufficiently long, and no significant improvement or detriment was observed with Gly_5 loops.

In summary, the monomeric variants we have designed fold into a structure that is closely similar to that of wild-type Rop, as evidenced by their high RNA-binding affinity. The monomeric variants are stable toward thermal denaturation and have a significant enthalpy associated with their thermal denaturation transition, consistent with the behavior of native-like proteins. The results suggest that the correct in-register association of the helices is sufficient to specify protein structure and that the connecting turns do not play an active role. This conclusion is consistent with the results of other studies on the effect of sequence variation in the turns of four-helix-bundle proteins (Brunet et al., 1993; Vlassi et al., 1994). It is important to emphasize, however, that although the correct association of helices appears to be dictated by the packing of the hydrophobic core, not all loop sequences are tolerated, and overall protein stability will be dependent to some extent on the length and sequence of the loops employed. The success of these simple redesigns of protein topology provides an encouraging precedent for similar manipulations of other proteins.

ACKNOWLEDGMENT

We thank Erin Duffy for help in creating the model for Rop_{S44} and Anna Lee and Don Crothers for discussions and generous gifts of RNA. We thank members of the Regan laboratory for critical reading of the manuscript and SUN Microsystems for computational support.

REFERENCES

Banner, D. W., Kokkinidis, M., & Tsernoglou, D. (1987) *J. Mol. Biol. 196*, 657−675.

Bird, R. E., Hardman, K. D., Jacobson, J. W., Johnson, S., Kaufman, B. N., Lee, S.-M., Lee, T., Pope, S. H., Riordan, G. S., & Whitlow, M. (1988) *Science 242*, 423−426.

Bizub, D., Weber, I. T., Cameron, C. E., Leis, J. P., & Skalka, A. M. (1991) *J. Biol. Chem. 266*, 4951−4958.

Bovia, F., Bui, N., & Strub, K. (1994) *Nucleic Acids Res. 22*, 2028−2035.

Brunet, A. P., Huang, E. S., Huffine, M. E., Loeb, J. E., Weltman, R. J., & Hecht, M. H. (1993) *Nature 364*, 355−358.

Brünger, A. T. (1992) *X-PLOR, version 3.1: A system for X-ray crystallography and NMR*, Yale University Press, New Haven, CT.

Eguchi, Y., & Tomizawa, J.-I. (1990) *Cell 60*, 199−209.

Eguchi, Y., & Tomizawa, J.-I. (1991) *J. Mol. Biol. 220*, 831−842.

Goldenberg, D. P., & Creighton, T. E. (1983) *J. Mol. Biol. 165*, 407−413.

Gregorian, R., & Crothers, D. M. (1995) *J. Mol. Biol.* (in press).

Hahn, M., Piotukh, K., Borriss, R., & Heinemann, U. (1994) *Proc. Natl. Acad. Sci. U.S.A. 91*, 10417−10421.

Ho, S. P., & DeGrado, W. F. (1987) *J. Am. Chem. Soc. 109*, 6751−6758.

Kraulis, P. J. (1991) *J. Appl. Crystallogr. 24*, 946−950.

Kreitman, R. J., Puri, R. K., & Pastan, I. (1994) *Proc. Natl. Acad. Sci. U.S.A. 91*, 6889−6893.

Liang, H., Sandberg, W. S., & Terwilliger, T. C. (1994) *Proc. Natl. Acad. Sci. U.S.A. 90*, 7010−7014.

Luger, K., Hommel, U., Herold, M., Hofsteenge, J., & Kirschner, K. (1989) *Science 243*, 206−210.

Munson, M., Predki, P. F., & Regan, L. (1994a) *Gene 144*, 59−62.

Munson, M., O'Brien, R., Sturtevant, J. M., & Regan, L. (1994b) *Protein Sci. 3*, 2015−2022.

Polisky, B. (1988) *Cell 55*, 929−932.

Predki, P. F., Nyak, L. M., Gottlieb, M. B. C., & Regan, L. (1995) *Cell 80*, 41−50.

Presnell, S., & Cohen, F. E. (1989) *Proc. Natl. Acad. Sci. U.S.A. 86*, 6592−6596.

Sander, C. (1990) *Biochem. Soc. Symp. 57*, 25−33.

Sanger, F., Nicklen, S., & Coulson, A. R. (1977) *Proc. Natl. Acad. Sci. U.S.A. 74*, 5463−5469.

Smith, C. K., Munson, M., & Regan, L. (1995) in *Techniques in Protein Chemistry VI* (Crabb, J. W., Ed.) pp 323−332, Academic Press, San Diego, CA.

Steif, C., Weber, P., & Hinz, H. J. (1993) *Biochemistry 32*, 3867−3876.

Toth, M. J., & Schimmel, P. (1986) *J. Biol. Chem. 261*, 6643−6646.

Vlassi, M., Steif, C., Weber, P., Tsernoglou, D., Wilson, K. S., Hinz, H.-J., & Kokkinidis, M. (1994) *Nature, Struct. Biol. 1*, 706−716.

Zhang, T., Bertelsen, E., Benvegnu, D., & Alber, T. (1993) *Biochemistry 32*, 12311−12318.

BI950979E